

Novel Biphasic Elastomeric Scaffold for Small-Diameter Blood Vessel Tissue Engineering

JIAN YANG, Ph.D., DELARA MOTLAGH, Ph.D., ANTONIO R. WEBB, B.E., and
GUILLERMO A. AMEER, Sc.D.

ABSTRACT

Compliance mismatch, thrombosis, and long culture times *in vitro* remain important challenges to the clinical implementation of a tissue-engineered small-diameter blood vessel (SDBV). To address these issues, we are developing an implantable elastomeric and biodegradable biphasic tubular scaffold. The scaffold design uses connected nonporous and porous phases as a basis to mimic, respectively, the intimal and medial layers of a blood vessel. Biphasic scaffolds were fabricated from poly(diols citrate), a novel class of biodegradable polyester elastomer. Scaffolds were characterized for tensile and compressive properties, burst pressure, compliance, foreign body reaction (via subcutaneous implantation in rats), and cell distribution and differentiation (via histology, scanning electron microscopy, and immunohistochemistry). Tensile tests, burst pressure, and compliance measurements confirm that the incorporation of a nonporous phase to create a “skin” connected to the porous phase of a scaffold can provide bulk mechanical properties that are similar to those of a native vessel. Compression tests confirm that the scaffolds are soft and recover from deformation. Subcutaneously implanted poly(diols citrate) porous scaffolds produce a thin fibrous capsule and allow for tissue ingrowth. *In vitro* culture of tubular biphasic scaffolds seeded with human aortic smooth muscle cells (HASMCs) and endothelial cells (HAECs) demonstrates the ability of this design to support cell compartmentalization, coculture, and cell differentiation. The newly formed HAEC monolayer stained positive for von Willebrand factor whereas collagen- and calponin-positive HASMCs were present in the porous phase.

INTRODUCTION

CARDIOVASCULAR DISEASE remains the leading cause of mortality in the United States, with approximately 1 million lives lost each year and healthcare-related costs exceeding 300 billion dollars.¹ Large-diameter (inner diameter, >5–6 mm) blood vessels have been successfully replaced with nondegradable polymeric materials such as Dacron (polyethylene terephthalate) and expanded polytetrafluoroethylene (ePTFE). Unfortunately, these materials are not applicable to small-diameter (inner diame-

ter, ≤ 5 mm) blood vessels, especially in locations below the knee. Poor patency is problematic due in part to incomplete endothelialization, thrombosis, and myointimal hyperplasia, particularly at the distal anastomosis.^{2,3} Both Dacron and ePTFE are relatively noncompliant compared with the elastic host blood vessel; therefore, it has been postulated that compliance mismatch may contribute to the development of myointimal hyperplasia. Several studies have suggested that the compliance of the graft should be similar to that of the blood vessel to be replaced, as both an undercompliant or overcompliant graft

may be detrimental for biomechanical adaptation.^{4–6} To date, no graft has successfully achieved long-term patency when used for small-diameter blood vessel (SDBV) applications. Therefore, the development of SDBV grafts has been an area of intense research focus.

Tissue-engineered blood vessels could potentially serve as an alternative source of grafts for patients. Significant progress has been made for the *in vitro* regeneration of SDBVs.^{7–12} L'Heureux and coworkers reported the fabrication of a completely biological human SDBV, which was produced by layering and wrapping sheets of cells around a mandrel, eliminating the use of exogenous scaffolds.¹⁰ Such constructs exhibited burst pressures that were comparable to that of native vessels (more than 2000 mmHg). However, the long *in vitro* processing time is a considerable limitation of this technology.⁷ Nerem and Seliktar⁸ and Niklason and coworkers⁹ used synthetic tubular poly(glycolic acid) (PGA) meshes to engineer SDBVs *in vitro* by means of a pulsatile perfusion system. The resulting constructs exhibited burst pressures higher than 2000 mmHg and desirable histological characteristics. Although these studies demonstrated the importance of mimicking *in vivo* mechanical conditions, PGA tubular scaffolds are not elastic and a silicone tube had to be used as a mandrel to transfer mechanical stimuli. Also, technical challenges such as relative sliding between the PGA tubular mesh and the silicone tube had to be addressed with the incorporation of Dacron sleeves. The PGA scaffold, which was initially seeded with smooth muscle cells, required long-term *in vitro* culture times in order to create a mechanically robust tissue equivalent before endothelial cells (ECs) could be seeded. The long-term culture time coupled with the removal of the silicone mandrel tube introduces increased risk of contamination and high costs.

Given the mechanically dynamic nature of blood vessels, scaffold mechanics are expected to be of utmost importance to the engineering of a blood vessel substitute.^{13,14} There are three major requirements for SDBV scaffolds: (1) biocompatibility and biodegradability; (2) structural similarity to the native blood vessel,^{15,16} as the scaffold should support adhesion, proliferation, and compartmentalization of smooth muscle cell (SMC) and EC functions; and (3) mechanical similarity to native blood vessels. First, ideal scaffolds should be soft and elastic. They should be able to sustain and recover from cyclic deformation without irritation to the surrounding tissues.^{17,18} Second, the compliance of the scaffolds should match the viscoelastic properties of the host vessel.^{19,20} Finally, for *in vivo* tissue engineering, scaffolds should be strong enough to withstand the hemodynamic forces exerted by the cardiovascular system and transfer mechanical stimulation to cells in an efficient manner in order to serve as a temporary blood conduit during tissue remodeling.⁹

With the increasing understanding of cellular and tissue reactions to vascular grafts, SDBV tissue engineering requires the development of novel scaffolds to move research closer to clinical application. In this regard, we set out to design a scaffold on the basis of the following premises: (1) an appropriate scaffold architecture should allow for simultaneous seeding of SMCs and ECs and facilitate the transfer of mechanical stimuli; (2) a cell-seeded scaffold with strong mechanical strength can potentially serve as a temporary vascular graft, thereby reducing the *in vitro* culture time to that required to achieve an EC monolayer (*in vivo* tissue engineering); and (3) a compliant scaffold with an inner functional monolayer of ECs should promote long-term patency. To address the above criteria, we have been developing a family of biodegradable elastomers referred to as poly(diols citrates) to engineer an elastomeric and biodegradable scaffold for tissue engineering SDBVs. Poly(diols citrates) are easy to synthesize, potentially cost-effective, and support the proliferation and differentiation of SMCs and ECs.^{21,22} In this work, we introduce a biphasic scaffold design and corresponding criteria that will be useful to vascular tissue-engineering efforts. A novel biphasic scaffold architecture was fabricated by sequential postpolymerization of concentric nonporous and porous layers of poly(diols citrates). The nonporous phase is expected to provide the following: (1) a continuous surface for EC adhesion, proliferation, and differentiation; and (2) mechanical strength and elasticity to the scaffold. The porous phase, polymerized directly onto the nonporous phase, is expected to facilitate the three-dimensional expansion and maturation of SMCs. The biphasic scaffold was evaluated via mechanical tests and cell culture experiments to assess its potential use for SDBV tissue engineering. The foreign body reaction to poly(diols citrate) scaffolds was also evaluated via subcutaneous implantation in rats.

MATERIALS AND METHODS

Poly(diols citrate) synthesis

All chemicals were purchased from Sigma-Aldrich (Milwaukee, WI). Citric acid was reacted with either C₈ or C₁₂ diols, creating poly(1,8-octanediol citrate) (POC) and poly(1,12-dodecanediol citrate) (PDDC). Various diols including aliphatic diols (C₆–C₁₂), *N*-methyl-diethanolamine (MDEA), and macrodiols such as poly(ethylene glycol) can also be used to create a polyester network with a controllable number of cross-links. Representatively, for POC synthesis,²¹ equimolar amounts of citric acid and 1,8-octanediol were added to a 250-mL three-neck round-bottom flask fitted with an inlet and outlet adapter. The mixture was melted at 160–165°C under a flow of nitro-

gen gas while stirring. The temperature of the system was subsequently lowered to 140°C for 30 min under stirring to create a prepolymer. The prepolymer was postpolymerized at either 60, 80, or 120°C under vacuum (2 Pa) or no vacuum for times ranging from 1 day to 2 weeks to create POC with various degrees of cross-linking.

Scaffold fabrication

Poly(diols citrate) nonporous tubes. Glass rods (~3 mm in diameter) were coated with the poly(diols citrate) prepolymer solution and air dried to allow for solvent evaporation. The thickness of the tube walls was controlled by the number of coatings and the percent prepolymer in the solution. After solvent evaporation for 24 h, the prepolymer-coated glass rods were transferred into a vacuum oven for postpolymerization. The resulting solid tubes were demolded by slightly swelling the tubes in 50% ethanol–water and vacuum dried for 48 h at room temperature.

Poly(diols citrate) porous scaffolds. Prepolymer was dissolved in 1,4-dioxane to form a 25 wt% solution, followed by addition of sieved salt, which served as a porogen. The resulting slurry was cast into poly(tetrafluoroethylene) (PTFE) molds (square or tubular shapes). After solvent evaporation for 24 h, the molds were transferred into an oven for postpolymerization (80°C, 4 days). The salt in the resulting composites was leached out by successive incubations in water (produced with a Milli-Q water purification system; Millipore, Billerica, MA) every 12 h for 96 h. The resulting porous spongelike films and tubular porous scaffolds were freeze-dried for 24 h and stored in a desiccator. The porosity of porous scaffolds was controlled by adjusting the ratio of polymer to salt and measured by a method based on Archimede's principle as described elsewhere.^{15,23} Scaffold cross-sections were observed by scanning electron microscopy (SEM) (S-3500N [Hitachi Science Systems, Ibaraki, Japan]; Electron Probe Instrumentation Center [EPIC], Northwestern University [Evanston, IL]) and images were analyzed with image analysis software (Image-Pro Plus, version 4.0; MediaCybernetics, Silver Spring, MD) to obtain the pore size data. At least 50 measurements were averaged.

Poly(diols citrate) biphasic scaffold. For the nonporous phase, a glass rod was coated with prepolymer and partially postpolymerized at 60°C for 24 h. To create the porous phase, the coated rod was inserted concentrically in a tubular mold that contained a salt–prepolymer slurry. The prepolymer–outer mold–glass rod system was then placed in an oven for further postpolymerization. After salt leaching, the biphasic tubular scaffold was demolded from the glass rod and freeze dried (Fig. 1). Biphasic scaffold cross-sections were observed by SEM.

Mechanical evaluation

Tensile tests. To investigate the effects of polymer processing on mechanical properties of scaffolds (80°C, 4 days), nonporous films, porous films (90% of porosity), and biphasic films (also referred to as scaffold) (90% porosity for porous phase) were made for tensile mechanical tests according to American Society for Testing and Materials (ASTM) 412a. The following samples were tested: POC films, PDDC films, POC porous films, PDDC porous films, biphasic scaffold with a PDDC porous phase and a PDDC nonporous phase, and biphasic scaffolds with a POC porous phase and a PDDC nonporous phase. Tests were performed on an Instron 5544 mechanical tester equipped with 500-N load cell (Instron, Norwood, MA). Briefly, dumbbell-shaped samples were pulled to failure at a rate of 500 mm/min. Ultimate tensile strength, Young's modulus, and elongation at break were obtained from stress–strain data. The thickness of porous and biphasic films was normalized to $T_{pf} \times (1 - \text{porosity})$ and $T_{pp} \times (1 - \text{porosity}) + T_{sp}$, respectively, where T_{pf} is the thickness of the porous film, T_{pp} is the thickness of the porous phase of the biphasic film, and T_{sp} is the thickness of the nonporous (solid) phase of the biphasic film.

Compressive tests. Mechanical properties of cylindrical porous POC (120°C, 2 Pa, 1 day) scaffolds (height, 6 mm; diameter, 6 mm; porosity, $90 \pm 2\%$; pore size, $106 \pm 26 \mu\text{m}$) were evaluated with an Instron 5544 mechanical tester at a cross-head speed of 2 mm min^{-1} and a 10-N load cell. To examine the elastic recovery properties, samples were compressed to one-fifth of their original length. The compressive modulus was obtained from the initial slope of the stress–strain data. After removing the compressive force, the recovery from deformation of the samples was measured with calipers. The compressive recovery ratio was expressed as follows: Recovery (%) = $L_1/L_0\%$, where L_1 and L_0 are the final and original length of the samples, respectively.

Burst pressure measurements. A syringe pump (Sage; Thermo Electron, Waltham, MA) with one 60-mL syringe was connected with Tygon tubing to one end of the sample tubes while the other end was affixed with tubing to a pressure gauge (Cole-Palmer Instrument, Vernon Hills, IL). The syringe pump was programmed to pump phosphate-buffered saline (PBS) at a rate of 0.67 mL/min

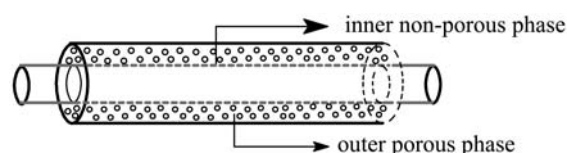


FIG. 1. Schematic of biphasic poly(diols citrate) scaffold.

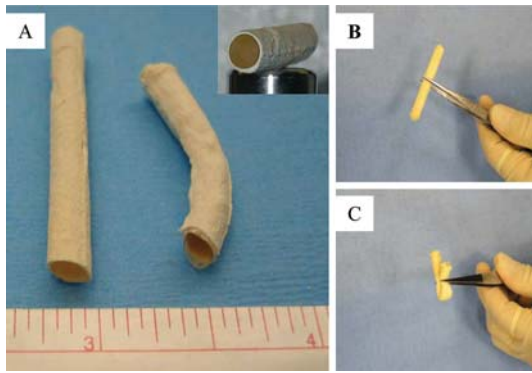


FIG. 2. (A–C) Soft biphasic scaffolds consisting of an inner nonporous lumen surrounded by an outer concentric porous layer. *Inset* in (A): A close look at the cross-section of a biphasic scaffold.

through the tube while pressure and time were recorded. The process to determine burst pressure was recorded with a video camera (NTSC ZR80; Canon, Tokyo, Japan). Burst pressures of solid poly(diols citrate) tubes (inner diameter, 3.65 mm) were defined as the highest pressure value attained before failure.

Compliance measurements. Compliance was defined as the change in diameter of a sample tube during the rise in pressure between diastole and systole (typically from 80 to 120 mmHg), and was expressed as a percentage. The volume of a sample tube at 80 mmHg (V_{80}) and 120 mmHg (V_{120}) was calculated on the basis of video camera data, recorded time, flow rate, and original tube volume. Compliance was expressed as $\Delta d/d$ (%) = $0.5(V_{120}/V_{80} - 1) \times 100$.²⁴

Foreign body reaction to implanted scaffolds

POC (120°C, 2 Pa, 3 days) porous scaffolds (diameter, 7 mm; thickness, 1.5 mm; pore size, $106 \pm 26 \mu\text{m}$; porosity, $90 \pm 2\%$) were sterilized by exposure to ethyl-

ene oxide gas, and subcutaneously implanted in the backs of 7-week-old female Sprague-Dawley rats, using blunt dissection. Rats were under deep isoflurane–O₂ general anesthesia. The rats were killed and tissue samples ($3 \times 3 \text{ cm}$) containing the implants were harvested at 7 and 30 days (three rats per time point). The samples were fixed in 10% formalin for 24 h and embedded in paraffin. Sections ($5 \mu\text{m}$) were stained with hematoxylin and eosin (H&E) for histological analysis. The foreign body reaction of the POC scaffolds was compared with that of porous poly(L-lactic acid) (PLLA) scaffolds (pore size, 60–90 μm ; porosity, $90 \pm 2\%$; $M_w > 300,000$; Poly-science, Warrington, PA) at 30 days.

Cell seeding and construct culture

Human aortic smooth muscle cells (HASMCs) and human aortic endothelial cells (HAECs) (Cambrex Bio Science Walkersville, Walkersville, MD) were cultured in a 50-mL culture flask with SmGM-2 and EBM-2 culture medium, respectively (Cambrex Bio Science Walkersville). Cell culture was maintained in a water-jacketed incubator (Forma Series II; Thermo Electron) equilibrated with 5% CO₂ at 37°C. Cells were not used beyond passage 5. All scaffolds for cell seeding were sterilized with ethylene oxide gas. HASMCs and HAECs were cocultured on POC biphasic scaffolds (both outer and inner phases are POC postpolymerized at 80°C, 3 days) using culture medium consisting of 3 parts SmGM-2 and 1 part EBM-2 (Cambrex Bio Science Walkersville). Briefly, one end of the scaffold was blocked and HAECs ($2.6 \times 10^5/\text{mL}$) were seeded into the lumen of the scaffold. The EC-seeded scaffold was placed in a culture dish (60 mm in diameter) containing EBM-2 medium. One day after EC seeding, the EBM-2 medium was removed carefully with a micropipette and HASMCs, at a density of $4 \times 10^6/\text{mL}$, were seeded onto the porous phase. The SMC- and EC-seeded scaffold was placed in the incubator for 30 min before adding 10 mL of coculture medium. The coculture medium was changed every 2 days. Porous

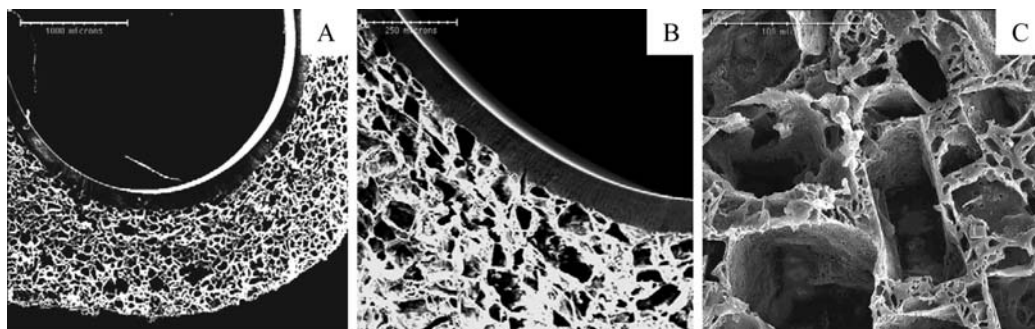


FIG. 3. (A) Cross-section of biphasic scaffold (POC porous phase and PDDC nonporous phase); (B) higher magnification of (A). (C) Pore structure of porous phase of biphasic scaffold. Scale bars: (A) 1000 μm ; (B) 250 μm ; (C) 100 μm .

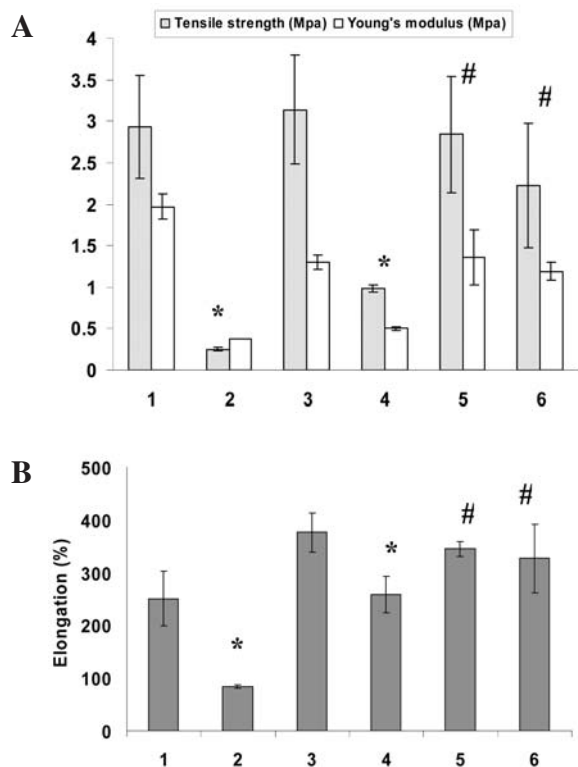


FIG. 4. Effects of scaffold processing on tensile strength and Young's modulus (**A**) and on elongation (**B**) of poly(diols citrate) scaffolds (80°C, 4 days) ($n = 4-6$). 1, POC film; 2, POC porous film; 3, PDDC film; 4, PDDC porous film; 5, biphasic scaffold with PDDC porous phase and nonporous phase; 6, biphasic scaffold with POC porous phase and PDDC nonporous phase. The porosity of the porous phase of both biphasic scaffolds was 90%. * $p < 0.05$, samples 2 and 4 compared with samples 1 and 2, respectively; # $p > 0.05$, samples 5 and 6 compared with sample 3.

scaffolds (nonbiphasic) were also directly seeded with HASMCs at a density of $4 \times 10^6/\text{mL}$.²¹ Constructs were cultured for up to 8 weeks.

SEM, histology, and immunohistochemistry

For SEM, biphasic scaffolds were fixed with 2.5% glutaraldehyde in PBS for 24 h at 4°C. After being thoroughly washed with PBS, the scaffolds were dehydrated sequentially in 50, 70, 95, and 100% ethanol, each three times (10 min each time). The fixed samples were freeze-dried, cut after freezing in liquid N₂, sputter coated with gold, and examined under an SEM (Hitachi S-3500N). For histology, the cell-cultured biphasic scaffolds were fixed in 10% buffered formalin (Sigma, St. Louis, MO), embedded in paraffin, sectioned into 8- to 10- μm slices, and stained with hematoxylin and eosin (H&E). For immunohistochemistry, sections of the cell-seeded scaffold were deparaffinized and immunostained for the presence of the SMC-specific protein, calponin. Briefly, mouse anti-calponin (Sigma) was

used at 1:10,000 dilution in blocking buffer consisting of 0.5% normal horse serum in PBS. Nonporous films seeded with ECs were fixed in 4% paraformaldehyde and immunostained for von Willebrand factor (vWF), a specific marker expressed by ECs. Rabbit anti-vWF (Santa Cruz Biotechnology, Santa Cruz, CA) was used at 1:500 dilution in 0.5% normal goat serum in PBS. Antibody-antigen complexes were visualized with a Vectastain ABC-AP kit (rabbit) for vWF and with a Vectastain Elite ABC kit (mouse) for calponin (Vector Laboratories, Burlingame, CA). Anti-mouse and anti-rabbit biotinylated secondary antibodies (diluted 1:200) were provided by the manufacturer. Calponin was visualized with a 3,3'-diaminobenzidine (DAB) substrate kit for peroxidase and von Willebrand factor was detected with a Vector blue substrate kit for alkaline phosphatase (Vector Laboratories).

Statistical analysis

Data were expressed as means \pm standard deviation. The statistical significance between two sets of data was calculated by two-tailed Student *t* test. Data were taken to be significant when a *p* value of 0.05 or less was obtained.

RESULTS

Scaffold fabrication

Despite the fact that cross-linked poly(diols citrates) are classified as thermoset polymers, in prepolymer form they can be processed into scaffolds of various shapes and porosities.²¹ A novel biphasic scaffold was fabricated with biodegradable poly(diols citrate). Biphasic tubular scaffolds consisted of an inner nonporous lumen surrounded by an outer concentric porous layer (Fig. 2A). The scaffolds were soft and could be bent repeatedly without permanent deformation or failure (Fig. 2B and C). The outer porous phase of the biphasic scaffold was chemically incorporated onto the nonporous phase via post-

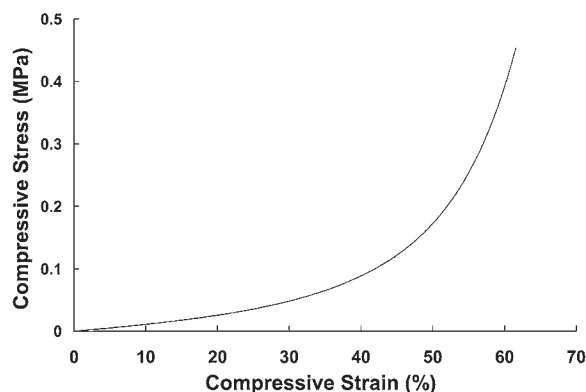


FIG. 5. Compressive mechanical tests on POC scaffolds, confirming that the scaffolds are soft.

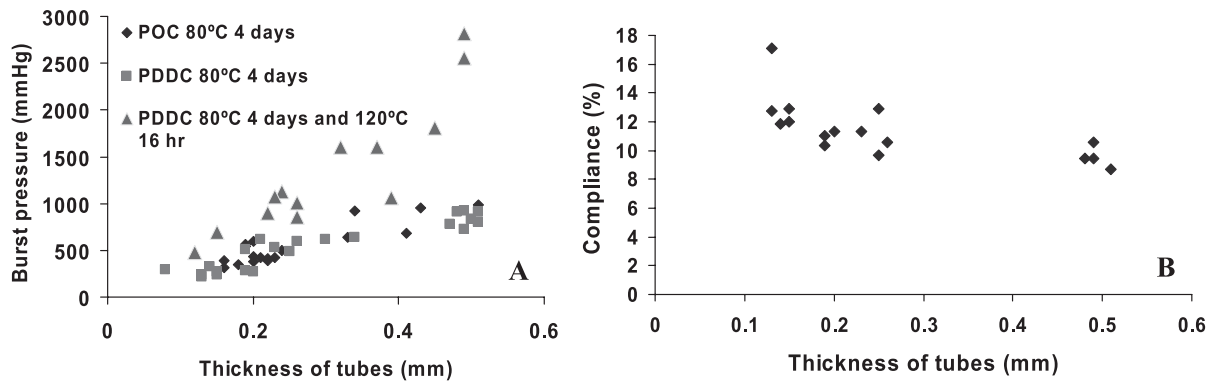


FIG. 6. (A) Burst pressure measurements of POC tubes synthesized under various postpolymerization conditions; (B) compliance measurements of PDDC tubes (80°C, 4 days) of various thickness.

polymerization (Fig. 3A and B). Micropores ($15 \pm 6 \mu\text{m}$) were distributed throughout the interconnected macropores and pore walls exhibited rough surfaces (Fig. 3C).

Mechanical evaluation

POC and PDDC porous films could maintain only 8.5 and 31.1%, respectively, of tensile strength (mean value) of corresponding nonporous films (Fig. 4A). There was a significant difference between the mechanical properties of nonporous and porous films ($p < 0.05$). On the other hand, PDDC-based and POC-based biphasic scaffolds

(samples 5 and 6; see Fig. 4A) maintained 90.2 and 70.7%, respectively, of tensile strength (mean value) relative to PDDC nonporous films. There was no statistically significant difference between the mechanical data for biphasic scaffolds and PDDC nonporous films ($p > 0.05$) (Fig. 4A and B). Figure 5 shows representative stress–strain data of POC scaffolds that were subjected to compression testing. The compressive modulus of the POC scaffold was $0.152 \pm 0.018 \text{ MPa}$. The small compressive modulus and tensile Young's modulus (Fig. 4A and 5) confirm that the scaffolds are soft. The scaffolds recovered to their original height (almost 100%) imme-

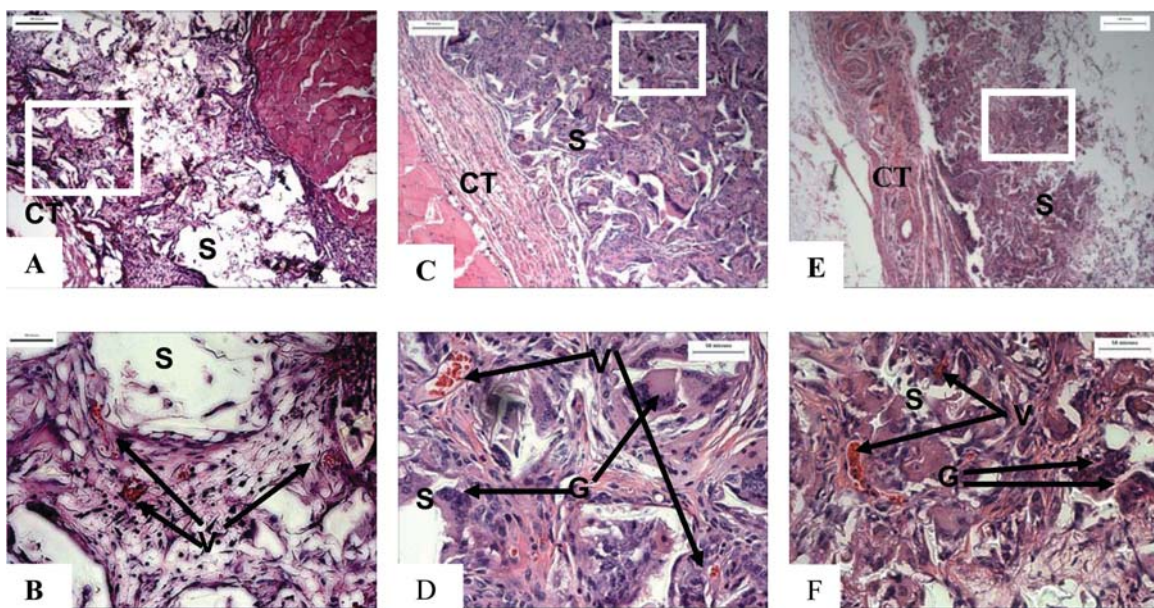


FIG. 7. H&E staining of porous POC (120°C, 2 Pa, 3 days) scaffolds and surrounding tissues after implantation for 7 days (A) and 30 days (C), and of a PLLA scaffold at 30 days (E). (B), (D), and (F) are enlargements of boxed areas in (A), (C), and (E), respectively. Scale bars: (A, C, and E) 200 μm ; (B, D, and F) 50 μm . S, scaffold (gray); V, blood vessel (arrows); G, giant cell (arrows); CT, connective tissue.

diately after the release of compressive forces. Burst pressure values of poly(diols citrate) nonporous tubes (Fig. 6A) exceeded that of typical systolic pressures (~ 120 mmHg). Burst pressure can be modulated by varying the thickness of the tube walls, postpolymerization conditions, and type of poly(diols citrate) used. Compliance of PDDC tubes (80°C ; 4 days; thickness, 0.16 mm) was 12.7%, which was similar to that of dog carotid (12.7%) and human carotid (14.7%).²⁴

Foreign body reaction to implanted scaffolds

After 7 days of implantation, significant fibrous tissue ingrowth occurred throughout the thickness of the scaffolds (Fig. 7A). Porous scaffolds were loosely encapsulated with a thin ($35 \pm 16 \mu\text{m}$) fibrous capsule. Inflammatory cells (macrophages) migrated into scaffolds from surrounding tissues and were distributed throughout the scaffolds. Many small blood vessels were found near the center of the scaffolds (Fig. 7B) and macrophages that surrounded the copolymer fragments exhibited a rounded shape. After 30 days of implantation, the scaffolds were filled with fibrous tissue and encapsulated with a thin anisotropic fibrous matrix (Fig. 7C). Capillary blood vessels were still present within the scaffolds and macrophages remained rounded. There was some evidence of giant cells around copolymer fragments (Fig. 7D). No tissue necrosis was observed at either time point. The foreign body reaction was essentially similar to that of PLLA porous scaffolds that were made via the salt-leaching method and also implanted in subcutaneous pockets on the backs of rats (Fig. 7E and F).

Cell seeding and construct culture

HASMCs seeded on porous POC stained positive for HASMC-specific calponin (brown) and surrounding collagen matrix (blue) (Fig. 8A and B). HAECs seeded on POC nonporous films were positive for von Willebrand factor (vWF) (blue) (Fig. 8C). Coculture of HASMCs and HAECs on biphasic scaffolds demonstrated that the biphasic scaffold design was able to compartmentalize both HASMCs and HAECs. Figure 9A shows a uniform HASMC distribution throughout the porous phase of the biphasic scaffold after 1 week in culture. HASMCs adhered to the pore walls through filopodial extensions, which are characteristic of three-dimensional attachment and proliferation, and secreted extracellular matrix (ECM) (Fig. 9C). HAECs proliferated to confluence on the nonporous phase (Fig. 9B).

DISCUSSION

The mechanical and microarchitectural characteristics of a blood vessel substitute are important in modulating

the phenotype of vascular cells, neotissue formation, and organization.^{2,25,26} In this article, we evaluate a novel biphasic scaffold design that takes into account scaffold mechanics (elasticity and strength) and cell compartmentalization requirements for tissue engineering a small-diameter blood vessel. An elastomeric scaffold is expected to better transmit dynamic mechanical stimuli exerted by a pulsatile bioreactor or the cardiovascular system if an *in vivo* tissue-engineering approach is implemented. Also, engineering the appropriate mechanics into the scaffold or blood vessel substitute should reduce compliance mismatch between the graft and host vessel, a biomechanical problem that has been cited as a factor contributing to graft failure.^{6,27,28} Most materials commonly used as scaffolds in vascular tissue engineering [i.e., polyglycolic acid, poly(lactide-co-glycolide), and others] lack elasticity and are prone to significant permanent deformation under cyclic mechanical stimulation.²⁹ The few synthetic elastomeric and biodegradable materials that have been explored, that is, polycaprolactone and copolymers thereof and poly(ester urethane)ureas,^{30,31} require complex synthesis schemes that include exogenous catalysts and are not cost-effective. Therefore, in our laboratory we developed a novel class of biodegradable polyester elastomers referred to as poly(diols citrates), which address the latter concerns and can be processed into scaffolds that are suitable for vascular tissue engineering. Poly(diols citrates) are condensation copolymers based on the reaction between citric acid and 1,*N*-aliphatic diols (typically C_8 , C_{10} , or C_{12}) or polyethylene glycols. The mechanical and biodegradation properties of poly(diols citrates) can be controlled by adjusting the feed ratio of citric acid to the chosen diol, by changing the type of diol, by adding trace amounts of cross-linking compounds such as glycerol and MDEA, or by changing postpolymerization conditions.^{21,22}

Regarding the microarchitectural requirements of a scaffold for vascular tissue engineering, facilitating or recreating the cell and extracellular matrix compartmentalization found in the native vessel wall could potentially lead to a more native-like vessel³² and also enable *in vivo* vascular tissue engineering. An ideal scaffold should provide the barrier function of the basement membrane for endothelial cell function and artificial elastic laminae for elasticity and separation between cell layers. We therefore set out to design and fabricate such a scaffold. The design, shown in Fig. 1, consists of a nonporous phase or skin within the lumen of an otherwise porous tubular scaffold. Postpolymerization of the outer porous phase directly in contact with the inner nonporous phase resulted in a continuous interface between both phases of the tubular scaffold, eliminating the potential for delamination (Fig. 3A). The porous phase of the biphasic scaffold was synthesized by particulate salt leaching and freeze-drying, which gave rise to a highly intercon-

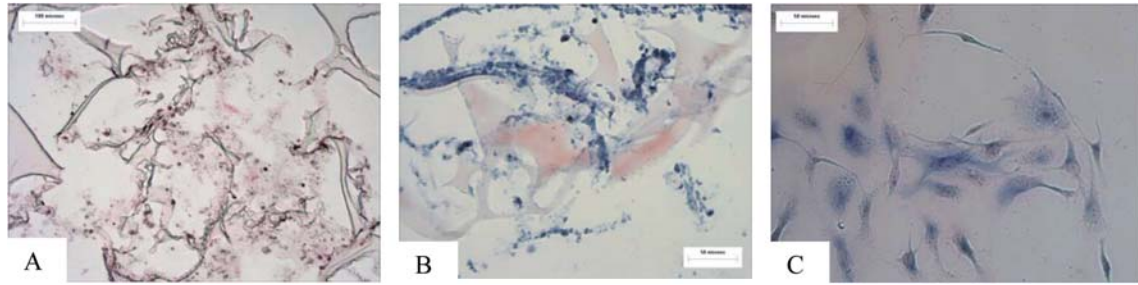


FIG. 8. (A) Immunostaining for the presence of SMC-specific protein calponin (brown) on a porous POC (80°C, 2 days) scaffold (8 weeks). Scale bar: 100 μm . (B) Masson's trichrome staining for total collagen (blue) on a porous POC (80°C, 2 days) scaffold (4 weeks). Scale bar: 50 μm . (C) Immunostaining for von Willebrand factor (blue) expressed by HAECs on POC (80°C, 4 days) film (3 days). Scale bar: 50 μm .

tive porous structure with micropore features along the macropore walls (Fig. 3C). The biphasic scaffold design would also allow rapid seeding and compartmentalization of SMCs and ECs, unlike current approaches that require long culture times for the *in vitro* growth and maturation of an SMC-based medial layer to enable EC seeding.^{9,33} The nonporous phase serves to mimic the barrier provided by the basement membrane for EC function and compartmentalization from SMCs. It also strengthens the porous phase and is expected to transduce mechanical stimulation to the SMCs located in the porous phase. In this respect, the biphasic scaffold had strength, modulus, and elongation values that were comparable to those of the nonporous films. The biphasic scaffold could potentially allow each cell type to receive its characteristic physiological mechanical stimulus (shear flow for ECs and circumferential and radial strain for SMCs and ECs). Therefore, the biphasic scaffold eliminates the need for a separate silicone tube to serve as a mandrel to conduct pulsatile mechanical stimuli to the surrounding porous scaffold. It also eliminates the need for “sleeves” to prevent relative sliding between the scaffold and an underlying silicone mandrel.

The effect of scaffold processing, that is, the incorporation of macropores, was evaluated by mechanical tests. Tensile tests performed on nonporous films, porous films, and biphasic films confirmed the utility of having a nonporous reinforcement in the lumen of a porous tube that would otherwise lose elasticity and strength because of the presence of high porosity (Fig. 4). The nonporous phase allows tailoring of the burst pressure and compliance of the biphasic scaffold in order to meet the requirements of the replaced vessels (Fig. 6A and B). Thus, the biphasic scaffold could potentially be used for *in vivo* vascular tissue engineering by providing a strong, compliant, and biodegradable blood flow conduit that can be remodeled by cells that were seeded *ex vivo*. As this approach would likely require only the culture of an EC monolayer to minimize or prevent thrombosis, *in vitro* culture time and expenses should be significantly reduced. In other words, a fully developed, *in vitro*-engineered medial layer is not required. The biphasic scaffold can also be used as a model scaffold to study the effect of scaffold compliance on new tissue formation during *in vitro* culture. Regarding recovery from deformation, the fast and complete recovery of porous scaffold

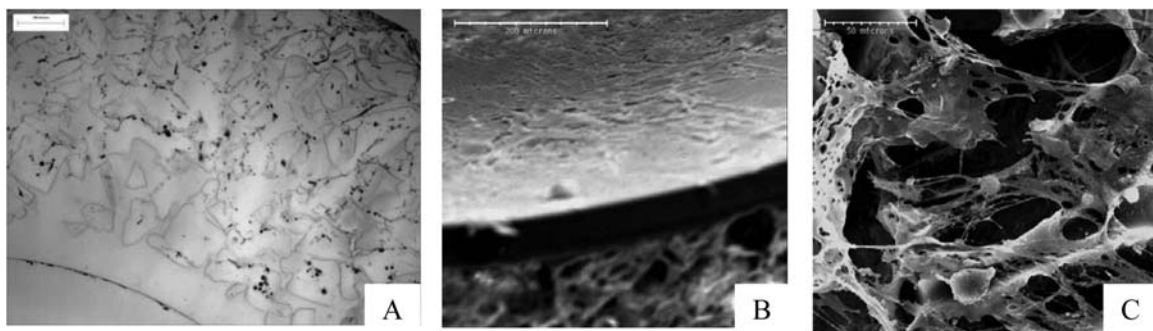


FIG. 9. HASMCs and HAECs cocultured on POC (80°C, 4 days) biphasic scaffolds (POC porous phase and POC nonporous phase). (A) H&E staining (1 week); (B) SEM picture of HAECs on the nonporous phase (lumen) of a biphasic scaffold (2 weeks); (C) SEM picture of HASMCs on the outer porous phase of a biphasic scaffold (2 weeks). Scale bars: 1 mm.

folds that were subjected to compressive forces suggests that permanent deformation should not be a significant concern.

The foreign body response to porous polydiol citrate scaffolds was comparable to that of porous PLLA scaffolds, a biodegradable polyester commonly used in tissue engineering (Fig. 7). Although biodegradable polyesters are not used for small-diameter blood vessel replacement in the clinical setting, comparison with PLLA was a first step to gain some insight into the relative biocompatibility of poly(diols citrates). The creation of a loosely packed, vascularized capsule instead of a well-organized avascular capsule depends on the shape of macrophages that interact with the implant. Round macrophages would favor the secretion of angiogenic factors.^{34,35} The significant fibrovascular tissue ingrowth after 1 week of implantation suggests that poly(diols citrate) scaffolds may be conducive to rapid angiogenesis and adaptation to the surrounding tissue. Fibrous encapsulation of the scaffold was maintained at a minimum throughout the 1-month period, which facilitates nutrient transport to the cells within the scaffold. The presence of giant cells along the pore walls suggests that cellular degradation of the scaffolds could potentially take place and should be considered as an additional degradation mechanism.³⁶ Future studies will evaluate the *in vivo* rate of degradation of various poly(diols citrate) scaffold combinations to obtain some better insight into their application in the body. The full ingrowth of fibrovascular tissue also confirmed the interconnectivity of the scaffolds (Fig. 7C).

The biphasic scaffold was able to compartmentalize both HASMCs and HAECs, as per the results of coculture experiments (Fig. 8). A confluent HAEC layer (Fig. 8B) was obtained on the nonporous phase of the biphasic scaffold. Histology and immunohistochemistry results demonstrated that HASMCs and HAECs seeded on porous scaffolds and nonporous films attained a differentiated phenotype and therefore have the potential to function as a tissue unit (Fig. 9). In the case of endothelial cells, a functional endothelium provides a continuous thromboresistant layer between blood and the blood vessel wall. It also controls blood flow and vessel tone, platelet activation, adhesion and aggregation, leukocyte adhesion, and SMC migration and proliferation.²⁰ Future studies will focus on the strength of adhesion and functionality of endothelial cells on poly(diols citrates). Several techniques, including surface coating,²⁰ controlled surface hydrolysis,^{37,38} immobilization of biomacromolecules,³⁹⁻⁴² and EC stress conditioning in culture,⁴³ have been proposed to improve cell adhesion for tissue-engineering scaffolds. Poly(diols citrate) scaffolds are amenable to all of the latter surface modification techniques to improve EC adhesion, if necessary.

In conclusion, a novel biphasic tubular scaffold consisting of connected nonporous and porous phases was fabricated and evaluated for potential use in vascular tissue engineering. The scaffold was made from poly(diols citrates), a new type of biodegradable polyester elastomer. These studies represent the first step toward the investigation of the role of scaffold mechanics in new tissue formation *in vitro* as well as *in vivo*. The biphasic scaffold could potentially be used to implement coculture of SMCs and ECs *in vitro*, thereby shortening culture time and reducing the risk of contamination. If the scaffold design is implemented for *in vivo* tissue engineering, it could potentially reduce the negative side effects associated with compliance mismatch between a graft and the host vessel, thereby improving long-term patency.

ACKNOWLEDGMENTS

This work was funded in part through grants from the American Heart Association and the National Institutes of Health (R21-HL071921-02). D.M. was funded by a BAXTER/IBNAM Early Career Development Award. The authors thank Marissa Darmoc for contributing the *in vivo* data for PLLA degradation.

REFERENCES

1. American Heart Association. 2005 Heart and Stroke Statistical Update. Dallas, TX: American Heart Association, 2005.
2. Xue, L., and Greisler, H.P. Biomaterials in the development and future of vascular grafts. *J. Vasc. Surg.* **37**, 472, 2003.
3. Niklason, L.E., and Langer, R.S. Advances in tissue engineering of blood vessels and other tissues. *Transplant. Immunol.* **5**, 303, 1997.
4. Tiwari, A., Cheng, K.S., Salacinski, H., Hamilton, G., and Seifalian, A.M. Improving the patency of vascular bypass grafts: The role of suture materials and surgical techniques on reducing anastomotic compliance mismatch. *Eur. J. Vasc. Endovasc. Surg.* **25**, 287, 2003.
5. Teebken, O.E., and Haverich, A. Tissue engineering a small diameter vascular grafts. *Eur. J. Vasc. Endovasc. Surg.* **23**, 475, 2002.
6. He, H., and Matsuda, T. Arterial replacement with compliant hierarchic hybrid vascular graft: Biomechanical adaptation and failure. *Tissue Eng.* **8**, 213, 2002.
7. Nerem, R.M., and Seliktar, D. Vascular tissue engineering. *Annu. Rev. Biomed. Eng.* **3**, 225, 2001.
8. Niklason, L.E., Gao, J., Abbott, W.M., Hirschi, K.K., Houser, S., Marini, R., and Langer, R. Functional arteries grown *in vitro*. *Science* **284**, 489, 1999.

9. Solan, A., Mitchell, S., Moses, M., and Niklason, L. Effect of pulse rate on collagen deposition in the tissue-engineered blood vessel. *Tissue Eng.* **9**, 579, 2003.
10. L'Heureux, N., Paquet, S., Labbe, R., Germain, L., and Auger, F.A. A completely biological tissue-engineered human blood vessel. *FASEB J.* **12**, 47, 1998.
11. Ye, Q., Zund, G., Benedikt, P., Jockenhoevel, S., Hoerstrup, S.P., Sakyama, S., Hubbell, J.A., and Turina, M. Fibrin gel as a three dimensional matrix in cardiovascular tissue engineering. *Eur. J. Cardiothorac. Surg.* **17**, 587, 2000.
12. Matsuda, T. Recent progress of vascular graft engineering in Japan. *Artif. Organs* **28**, 64, 2004.
13. Nerem, R.M., and Stegeman, J.P., Functional requirements for the engineering of a blood vessel substitute. In: Guilak, F., Butler, D.L., Goldstein, S.A., and Mooney, D.J., eds. *Functional Tissue Engineering*. New York: Springer-Verlag, 2003, p. 87.
14. Kim, B.S., Jeong, S.I., Cho, S.W., Nikolovski, J., Mooney, D.J., Lee, S.H., Jeon, O., Kim, T.W., Lim, S.H., Hong, Y.S., Choi, C.Y., Lee, Y.M., Kim, S.H., and Kim, Y.H. Tissue engineering of smooth muscle under a mechanically dynamic condition. *J. Microbiol. Biotechnol.* **13**, 841, 2003.
15. Widmer, M.S., Gupta, P.K., Lu, L.C., Meszlenyi, R.K., Evans, G.R.D., Brandt, K., Savel, T., Gurlek, A., Patrick, C.W., and Mikos, A.G. Manufacture of porous biodegradable polymer conduits by an extrusion process for guided tissue engineering. *Biomaterials* **19**, 1945, 1998.
16. Hubbell, J.A. Materials as morphogenetic guide in tissue engineering. *Curr. Opin. Biotechnol.* **14**, 551, 2003.
17. Wang, Y., Ameer, G.A., Sheppard, B., and Langer, R. A tough biodegradable elastomer. *Nat. Biotechnol.* **20**, 587, 2002.
18. Thornton, A.J., Alsberg, E., Albertelli, M., and Mooney, D.J. Shape-defining scaffolds for minimally invasive tissue engineering. *Transplantation* **77**, 1789, 2004.
19. Salacinski, H.J., Goldner, S., Giudiceandrea, A., Edwards, A., Hamilton, G., and Seifalian, A.M. The mechanical behavior of vascular grafts: A review. *J. Biomater. Appl.* **15**, 241, 2001.
20. Seifalian, A.M., Tiwari, A., Hamilton, G., and Salacinski, H.J. Improving the clinical patency of prosthetic vascular and coronary bypass grafts: The role of seeding and tissue engineering. *Artif. Organs* **26**, 307, 2001.
21. Yang, J., Webb, A.R., and Ameer, G.A. Novel citric acid-based biodegradable elastomers for tissue engineering. *Adv. Mater.* **16**, 511, 2004.
22. Webb, A.R., Yang, J., and Ameer, G.A. Biodegradable polyester elastomers in tissue engineering. *Expert Opin. Biol. Ther.* **4**, 801, 2004.
23. Yang, J., Shi, G.X., Bei, J.Z., Wang, S.G., Cao, Y.L., Shang, Q.X., Yang, G.H., and Wang, W.J. Fabrication and surface modification of macroporous poly(L-lactic acid) and poly(L-lactic-co-glycolic acid) (70/30) cell scaffolds for human skin fibroblast cells culture. *J. Biomed. Mater. Res.* **62**, 438, 2002.
24. Roeder, R., Wolfe, J., Lianakis, N., Hinson, T., Geddes, L.A., and Obermiller, J. Compliance, elastic modulus, and burst pressure of small-intestine submucosa (SIS), small-diameter vascular grafts. *J. Biomed. Mater. Res.* **47**, 65, 1999.
25. Stegeman, J.P., and Nerem, R.M. Phenotype modulation in vascular tissue engineering using biochemical and mechanical stimulation. *Ann. Biomed. Eng.* **31**, 391, 2003.
26. Niklason, L.E., Abbott, W., Gao, J., Klagges, B., Hirschi, K., Ulubayram, K., Conroy, N., Jones, R., Vasanwala, A., Sanzgeri, S., and Langer, R. Morphologic and mechanical characteristics of engineered bovine arteries. *J. Vasc. Surg.* **33**, 628, 2001.
27. Berry, J.L., Manoach, E., Mekkaoui, C., Rolland, P.H., Moore, J.E., and Rachev, A. Hemodynamics and wall mechanics of a compliance matching stent: *In vitro* and *in vivo* analysis. *J. Vasc. Interv. Radiol.* **13**, 97, 2002.
28. Knez, P., Nelson, K., Hakimi, M., Al-Haidary, J., Schneider, C., and Schmitz-Rixen, T. Rotational *in vitro* compliance measurement of diverse anastomotic configurations: A tool for anastomotic engineering. *J. Biomech.* **37**, 275, 2004.
29. Kim, B.S., and Mooney, D.J. Scaffolds for engineering smooth muscle under cyclic mechanical strain conditions. *J. Biomech. Eng.* **122**, 210, 2000.
30. Jeong, S.I., Kim, S.H., Kim, Y.H., Jung, Y.M., Kwon, J.H., and Kim, B.S. Manufacture of elastic biodegradable PLCL scaffolds for mechano-active vascular tissue engineering. *J. Biomater. Sci. Polym. Ed.* **15**, 645, 2004.
31. Guan, J., Michael, S.S., Beckman, E.J., and Wagner, W.R. Synthesis, characterization, and cytocompatibility of elastomeric, biodegradable poly(ester-urethane)ureas based on poly(caprolactone) and putrescine. *J. Biomed. Mater. Res.* **61**, 493, 2002.
32. Ma, P.X., and Zhang, R. Microtubular architecture of biodegradable polymer scaffolds. *J. Biomed. Mater. Res.* **56**, 469, 2001.
33. Nasserli, B.A., Pomerantseva, I., Kaazempur-Mofrad, M.R., Sutherland, F.W.H., Perry, T., Ochoa, E., Thompson, C.A., Mayer, J.E., Oesterle, S.N., and Vacanti, J.P. Dynamic rotational seeding and cell culture system for vascular tube formation. *Tissue Eng.* **9**, 291, 2003.
34. Sieminski, A.L., and Gooch, K.J. Biomaterial-microvasculature interactions. *Biomaterials* **21**, 2233, 2000.
35. Padera, R.F., and Colton, C.K. Time course of membrane microarchitecture-driven neovascularization. *Biomaterials* **17**, 277, 1996.
36. van Tienen, T.G., Heijkants, R.G.J.C., Buma, P., de Groot, J.H., Pennings, A.J., and Veth, R.P.H. Tissue ingrowth and degradation of two biodegradable porous polymers with different porosities and pore sizes. *Biomaterials* **23**, 1731, 2002.
37. Yang, J., Wan, Y., Tu, C., Cai, Q., Bei, J., and Wang, S. Enhancing the cell affinity of macroporous poly(L-lactide) cell scaffold by a convenient modification method. *Polym. Int.* **52**, 1892, 2003.
38. Gao, J., Niklason, L., and Langer, R. Surface hydrolysis of poly(glycolic acid) meshes increases the seeding density of vascular smooth muscle cells. *J. Biomed. Mater. Res.* **42**, 417, 1998.
39. Yang, J., Bei, J., and Wang, S. Enhanced cell affinity of poly(D,L-lactide) by combining plasma treatment with collagen anchorage. *Biomaterials* **23**, 2607, 2002.

40. Yang, J., Wan, Y.Q., Yang, J.L., Bei, J.Z., and Wang, S.G. Plasma treated, collagen anchored polylactone: Its cell affinity evaluation under shear or shear free conditions. *J. Biomed. Mater. Res.* **67A**, 1139, 2003.
41. Zhu, Y., Gao, C., Liu, X., He, T., and Shen, J. Immobilization of biomacromolecules onto aminolyzed poly(L-lactic acid) toward acceleration endothelium regeneration. *Tissue Eng.* **10**, 53, 2004.
42. Rowley, J.A., Sun, Z., Goldman, D., and Mooney, D.J. Biomaterials to spatially regulate cell fate. *Adv. Mater.* **14**, 886, 2002.
43. Carnagey, J., Hern-Anderson, D., Ranieri, J., and Schmidt, C.E. Rapid endothelialization of PhotoFix natural biomaterial vascular grafts. *J. Biomed. Mater. Res.* **65B**, 171, 2002.

Address reprint requests to:
Guillermo A. Ameer, Sc.D.
Department of Biomedical Engineering
Northwestern University
Evanston, IL 60208

E-mail: g-ameer@northwestern.edu